

# Controlling Geometry of Homology Generators

**Abstract** Homology groups and their generators of a 2D image are computed using a hierarchical structure i.e. irregular graph pyramid. In this paper we show that the generators of the first homology groups of a 2D image, computed with this pyramid based method always fit on the boundaries of the regions.

## 1 Introduction

A region/object is a (structured) set of pixels or voxels, or more generally a (structured) set of lower-level regions. At the lowest level of abstraction, such an object is a subdivision, i.e. a partition of the object into cells of dimensions 0, 1, 2, 3 ... (i.e. vertices, edges, faces, volumes ...) [13]. In general, combinatorial structures (graphs, combinatorial maps, nG-maps etc.) are used to describe objects subdivided into cells of different dimensions. The structure of the object is related to the decomposition of the object into sub-objects, and to the relations between these sub-objects: basically, topological information is related to the cells and their adjacency or incidence relations. Further information (embedding information) is associated to these sub-objects, and describes for instance their shapes (e.g. a point, respectively a curve, a part of a surface, is associated with each vertex, respectively each edge, each face), their textures or colors, or other information depending on the application. A common problem is to characterize structural (topological) properties of handled objects. Different topological invariants have been proposed like Euler characteristics, orientability, homology... (see [1]).

Homology is a powerful topological invariant, which characterizes an object by its " $p$ -dimensional holes". Intuitively 0-dimensional holes can be seen as connected components, 1-dimensional holes can be seen as tunnels and 2-dimensional holes as cavities. Unfortunately, there are no English notions for higher dimensional holes. This notion of  $p$ -dimensional hole is defined in any dimension. In Fig.1(a) an example of the torus is shown, which contains one 0-dimensional hole, two 1-dimensional holes (each of them are an edge cycle) and one 2-dimensional hole (the cavity enclosed by the entire surface of the torus). Plainly, homology is a tool to study digital spaces, and has been applied for 2D and 3D image analysis [2]. Usage of homology groups and generators is a new topic and has been recently

used in image processing. Although in this paper we use 2D images to show some nice properties of using homology groups and their generators in studying images, we do not encourage usage of homology groups and generators to find connected components in 2D image, since efficient approaches already exist [19]. However, these 'classical' approaches cannot be easily extended for many problems that exist in higher dimensions, since our visual intuition is inappropriate and topological reasoning becomes important. Computational topology has been used in metallurgy [9] to analyze 3D spatial structure of metals in an alloy and in medical image processing [17] in analyzing blood vessels. In higher dimensional problems (e.g. beating heart represented in 4D) the importance of homology groups and generators becomes clear in analyzing objects (their number of connected components, tunnels, holes, etc) in these spaces, because of the nice and clean formulations which hold in any dimension.

Moreover, if Betti numbers (rank of homology groups) provide the number of " $p$ -dimensional" holes, a set of generators allows to locate them. In [18], it is shown that different parameters influence the geometry of the generators i.e. a generator can surround a " $p$ -hole" more or less closely. A new method for computing homology groups and their generators is introduced in [5]. It uses a hierarchical structure based on a graph pyramid which is build by using two operations: contraction and removal. The main goal of this paper is to show that the generators build by the method in [5] is on the boundaries of the regions. We show this property by experimenting using 2D images and conjecture that this properties will hold also for higher dimensional data.

The paper is structured as follows. Basic notions of homology and irregular graph pyramids are recalled in Section 2 and 3. The new method to compute homology groups and their generators is presented in detail in Section 4. We finally show some experimental results on 2D images in Section 6.

## 2 Homology

In this part, the basic homology notions of chain, cycle, boundary and homology generator are recalled, interested readers can find more details in [16].

The homology of a subdivided object  $X$  can be defined in an algebraic way by studying incidence relations of its

121  
122  
123  
124  
125  
126  
127  
128  
129  
130  
131  
132  
133  
134  
135  
136  
137  
138  
139  
140  
141  
142  
143  
144  
145  
146  
147  
148  
149  
150  
151  
152  
153  
154  
155  
156  
157  
158  
159  
160  
161  
162  
163  
164  
165  
166  
167  
168  
169  
170  
171  
172  
173  
174  
175  
176  
177  
178  
179  
180

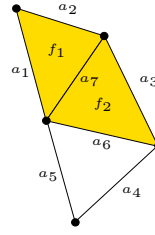
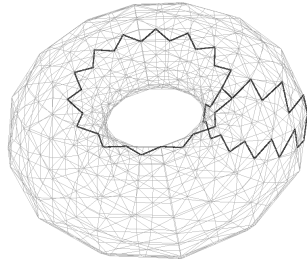


**Figure 1:** (a) : a triangulation of the torus. (b) : a simplicial complex made of 1 connected component and containing one 1–dimensional hole.

subdivision. Within this context, a cell of dimension  $p$  is called a  $p$ –cell and the notion of  $p$ –chain is defined as a sum  $\sum_{i=1}^{nb} \alpha_i c_i$ , where  $c_i$  are  $p$ –cells of  $X$  and  $\alpha_i$  are coefficients assigned to each cell in the chain. Homology can be computed using any group  $\mathcal{A}$  for the coefficients  $\alpha_i$ . Anyway, the theorem of universal coefficients [16] ensures that all homological information is obtain by choosing  $\mathcal{A} = \mathbb{Z}$ . It is also known [16] that for nD objects embedded in  $\mathbb{R}^D$  the homology information can be computed considering simply chains with moduli 2 coefficients ( $\mathcal{A} = \mathbb{Z}/2\mathbb{Z}$ ). Note that is this case, a cell that appears twice on a chain vanishes, because  $c + c = 0$  for any cell  $c$  when using moduli 2 coefficients. On the following, only chains with coefficients over  $\mathbb{Z}/2\mathbb{Z}$  will be considered.

Note that the notion of chain is purely formal and the cells that compose a chain do not have to satisfy any property. For example, on the simplicial complex illustrated on Fig.1(b) the sums:  $a_1 + a_4$ ,  $a_3$  and  $a_2 + a_7 + a_4$  are 1–chains.

For each dimension  $p = 0, \dots, n$ , where  $n = \dim(X)$ , the set of  $p$ –chains forms an abelian group denoted  $C_p$ . The  $p$ –chain groups can be put into a sequence, related by applications  $\partial_p$  describing the boundary of  $p$ –chains as  $(p - 1)$ –chains:

$$C_n \xrightarrow{\partial_n} C_{n-1} \xrightarrow{\partial_{n-1}} \dots \xrightarrow{\partial_1} C_0 \xrightarrow{\partial_0} 0,$$

which satisfy  $\partial_p \partial_{p-1}(c) = 0$  for any  $p$ –chain  $c$ ,  $p = 1..n$ . This sequence of groups is called a *free chain complex*.

The boundary of a  $p$ –chain reduced to a single cell is defined as the sum of its incident  $(p - 1)$ –cells. The boundary of a general  $p$ –chain is then defined by linearity as the sum of the boundaries of each cell that appears in the chain e.g. in Fig.1(b),  $\partial(f_1 + f_2) = \partial(f_1) + \partial(f_2) = (a_1 + a_2 + a_7) + (a_7 + a_3 + a_6) = a_1 + a_2 + a_3 + a_6$ . Note that as mentioned before, chains are considered over  $\mathbb{Z}/2\mathbb{Z}$  coefficients, any cell that appears twice vanishes.

For each dimension  $p = 0 \dots n$ , the set of  $p$ –chains which have a null boundary are called  $p$ –cycles and are a subgroup of  $C_p$ , denoted  $Z_p$  e.g.  $a_1 + a_2 + a_7$  and  $a_7 + a_5 + a_4 + a_3$  are 1–cycles. The set of  $p$ –chains which bound a  $p + 1$ –chain are called  $p$ –boundaries and they are a subgroup of  $C_p$ , denoted  $B_p$  e.g.  $a_1 + a_2 + a_7 = \partial(f_1)$  and  $a_1 + a_6 + a_3 + a_2 = \partial(f_1 + f_2)$  are 1–boundaries.

According to the definition of a free chain complex, the boundary of a boundary is the null chain. Hence, this implies that any boundary is a cycle. Note that according to the

definition of a free chain complex, any 0–chain has a null boundary, hence every 0–chain is a cycle.

The  $p^{th}$  homology group, for  $p = 0 \dots n$ , denoted  $H_p$ , is defined as the quotient group  $Z_p/B_p$ . Thus, elements of the homology groups  $H_p$  are equivalence classes and two cycles  $z_1$  and  $z_2$  belong to the same equivalence class if their difference is a boundary ( i.e.  $z_1 = z_2 + b$ , where  $b$  is a boundary). Such two cycles are called *homologous* e.g. let  $z_1 = a_5 + a_4 + a_3 + a_7$ ,  $z_2 = a_5 + a_4 + a_6$  and  $z_3 = a_1 + a_2 + a_3$ ;  $z_1$  and  $z_2$  are homologous ( $z_1 = z_2 + \partial(f_2)$ ) but  $z_1$  and  $z_2$  are not homologous to  $z_3$ . Let  $H_p$  be an homology group generated by  $q$  independent equivalence classes  $C_1, \dots, C_q$ , any set  $\{h_1, \dots, h_q \mid h_1 \in C_1, \dots, h_q \in C_q\}$  is called a *set of generators* for  $H_p$ . For example, either  $\{z_1\}$ ,  $\{z_2\}$  can be chosen as a generator of  $H_1$  for the object represented in Fig.1(b).

Note that some notions mentioned above can be confusing with similar notions in the graph theory field. Tab.1 associates these homology with notions classically used in graph theory.

### 3 Irregular Graph Pyramids

In this part, basic notions of pyramids like receptive field, contraction kernel, and equivalent contraction kernel are introduced, for more details see [8].

A pyramid (Fig. 2(a) describes the contents of an image at multiple levels of resolution. A high resolution input image is at the base level. Successive levels reduce the size of the data by *reduction factor*  $\lambda > 1.0$ . The *Reduction window* relates one cell at the reduced level with a set of cells in the level directly below. The contents of a lower resolution cell is computed by means of a *reduction function* the input of which are the descriptions of the cells in the reduction window. Higher level descriptions should be related to the original input data in the base of the pyramid. This is done by the *receptive field* (RF) of a given pyramidal cell  $c_i$ . The  $RF(c_i)$  aggregates all cells (pixels) in the base level of which  $c_i$  is the ancestor.

Each level represents a partition of the pixel set into cells, i.e. *connected subsets of pixels*. The construction of an irregular pyramid is iteratively local [15]. On the base level (level 0) of an irregular pyramid the cells represent single pixels and the neighborhood of the cells is defined by the 4(8)-connectivity of the pixels. A cell on level  $k + 1$  (parent) is a union of some neighboring cells on level  $k$  (child)

181  
182  
183  
184  
185  
186  
187  
188  
189  
190  
191  
192  
193  
194  
195  
196  
197  
198  
199  
200  
201  
202  
203  
204  
205  
206  
207  
208  
209  
210  
211  
212  
213  
214  
215  
216  
217  
218  
219  
220  
221  
222  
223  
224  
225  
226  
227  
228  
229  
230  
231  
232  
233  
234  
235  
236  
237  
238  
239  
240

**Table 1:** Translation of homology notions in the graph field.

Homology theory	Graph theory
0-cell, 1-cell, 2-cell	vertex, edge, face
0-chain, 1-chain, 2-chain	set of vertices, set of edges, set of faces
0-cycle, 1-cycle, 2-cycle	set of vertices, closed path of edges, closed path of faces

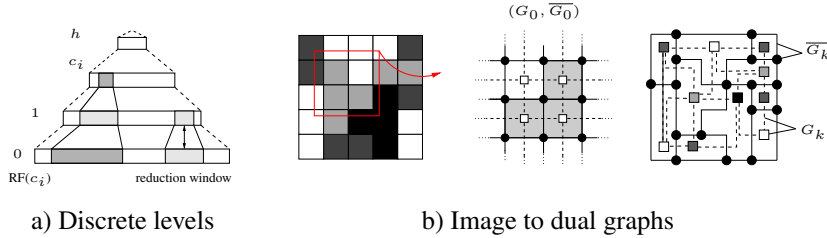


**Figure 2:** (a) pyramid concept, and (b) representation of the cells and their neighborhood relations by a dual pair of plane graphs at the level 0 and  $k$  of the pyramid.

dren). This union is controlled by so called *contraction kernels* (CK) [14], a spanning forest which relate two successive level of a pyramid. Every parent computes its values independently of other cells on the same level. Thus local independent (and parallel) processes propagate information up and down and laterally in the pyramid. Neighborhoods on level  $k + 1$  are derived from neighborhoods on level  $k$ . Higher level description are related to the original input by the *equivalent contraction kernels* (ECK). A level of the graph pyramid consists of a pair  $(G_k, \overline{G}_k)$  of plane graphs  $G_k$  and its geometric dual  $\overline{G}_k$  (Fig. 2(b)). The vertices of  $G_k$  represent the cells on level  $k$  and the edges of  $G_k$  represent the neighborhood relations of the cells, depicted with square vertices and dashed edges in Fig. 2(b). The edges of  $\overline{G}_k$  represent the borders of the cells on level  $k$ , solid lines in Fig. 2(b), including so called pseudo edges needed to represent neighborhood relations to a cell completely enclosed by another cell. Finally, the vertices of  $\overline{G}_k$  (circles in Fig. 2(b)), represent junctions of border segments of  $\overline{G}_k$ . The sequence  $(G_k, \overline{G}_k)$ ,  $0 \leq k \leq h$  is called irregular (dual) graph pyramid. For simplicity of the presentation the dual  $\overline{G}$  is omitted afterward.

## 4 Computing Homology Generators

There exists a general method for computing homology groups. This method is based on the transformation of incidence matrices [16] (i.e. which describe the boundary homomorphisms) into their reduced form called *Smith normal form*. Agoston proposes a general algorithm, based on the use of slightly modified Smith normal form, for computing a set of generators of these groups [1]. Even if Agoston's algorithm is defined in any dimension, the main drawback of this method is directly linked to the complexity of the reduction of an incidence matrix into its Smith normal form, which is known to consume a huge amount of time and space. Another well known problem is the possible appearance of huge integers during the reduction of the matrix. A more complete discussion about Smith normal algorithm complexity can be found in [12]. Indeed, Agoston's algorithm cannot directly be used for computing

homology generators and different kinds of optimisations have been proposed.

Based on the work of [4] and [20], an optimisation for the computation of homology generators, based on the use of sparse matrices and moduli operations has been proposed [18]. In particular, this method avoids the possible appearance of huge integers. The authors also observed an improvement of time complexity dropping from  $O(n^2)$  to  $O(n^{5/3})$ , where  $n$  is the number of cells of the subdivision.

An algorithm for computing the rank of homology groups i.e. the Betti numbers have been proposed in [11]. The main idea of this algorithm is to reduce the number of cells of an initial object in order to obtain an homologically equivalent object, made of less cells. In some special cases (orientable objects), Betti numbers can directly be deduced from the resulting object. However, this method cannot directly provide a set of generators. Based on this work, an algorithm for computing a minimal representation of the boundary of a 3D voxel region, from which homology generators can directly be deduced have been defined in [3].

### 4.1 Generator Computation using Pyramids (GCP)

The GCP method proposed in [5] follows the same idea as the methods of Kaczynski and Damiand [10, 6]: reducing the number of cells of an object for computing homology. Moreover, we keep all simplifications that are computed during the reduction process by using the pyramid. In this way, homology generators can be computed at the top level of the pyramid, and can be used to deduce generators of any lower level of the pyramid. The generators of the higher level can be directly down-projected on the desired level (using equivalent contraction kernels).

Starting from an initial image, an irregular graph pyramid is build. This method is valid as long as the algorithm used for the construction of the pyramid preserves homology. In particular, it is shown in [5] that the decimation by contraction kernels, described in section 3, preserves homology. Indeed, homology of the initial image can thus be computed in any level of the pyramid, and in particular on the top level

361 where the object is described with the smallest number of  
 362 cells.

364 The GCP method is summarized into the following steps:

- 366 1 Starting from labeled image, a graph pyramid  
 367  $\{G_0, G_1, \dots, G_k\}$  is built using contraction kernels  
 368 of cells with the same label.
- 369 2 Homology groups generators are computed for  $G_k$ , using  
 370 Agoston's method.
- 371 3 Homology generators of any level  $i$  can be deduced from  
 372 those of level  $i + 1$  using the contraction kernels. In par-  
 373 ticular, we obtain the homology generators of the initial  
 374 image.  
 375  
 376

377 Fig.3 illustrates the general method that we propose for  
 378 computing homology generators of an image.

## 380 5 Controlling the Geometry of the 381 Generators

383 When computing homology generators with Agoston's  
 384 method, directly on the initial image, we cannot have any  
 385 control of their geometry. More precisely, the aspect of the  
 386 obtained generators is directly linked to the construction of  
 387 incidence matrices, which is determined by the scanning  
 388 of each cell of the initial image (see [18] for a first study  
 389 of the influence of different parameters on the geometry of  
 390 generators).

391 We prove in this section that for 2D images, the GCP  
 392 method provides a set of generators that always fit on some  
 393 boundaries of a region  $R$ . In the following, an edge on the  
 394 boundary of a region is called a boundary edge.

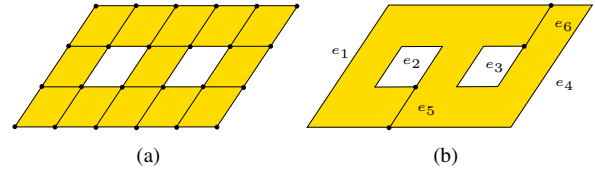
395 First, we show that any 1-cycle in the top level of the  
 396 pyramid computed with GCP method contains only bound-  
 397 ary edges. Second, we show that the down-projection of a  
 398 1-cycle composed of boundary edges, is still a cycle com-  
 399 posed of boundary edges.

401 **Property 1** Any 1-cycle in the top level of the pyramid  
 402 computed with GCP method contains only boundary edges

404 **Proof:** On the top level, a region is represented by a unique  
 405 2D cell. Hence each edge of the top level is either a bound-  
 406 ary edge or links two boundaries of  $R$  (we call it a pseudo  
 407 edge).

408 Let  $z$  be a 1-cycle on the top level, if  $z$  contains any  
 409 pseudo edge  $e = (v_1, v_2)$ , where  $v_1$  and  $v_2$  are two ver-  
 410 tices that stand on two different boundaries of  $R$ , then  $R$   
 411 is made of at least two 2D-cells, which is not possible as any  
 412 region on the top level is made of only one cell. Hence,  
 413 any 1-cycle on the top level of the pyramid contains only  
 414 boundary edges.  
 415  $\square$

416 Let us consider Fig. 4(b), which represents the top level  
 417 of the pyramid built from the initial image represented in  
 418 Fig. 4(a). The subdivision is made of one 2D-cell  $R_1$ ; four  
 419 boundary edges  $e_1, e_2, e_3, e_4$ ; two pseudo edges  $e_5, e_6$ ; and



421 **Figure 4:** (a) Bottom level, and (b) top level of the pyramid.

422 four vertices. The property 1 ensures that for this subdivi-  
 423 sion, any 1-cycle can be written as  $\alpha_1 e_1 + \alpha_2 e_2 + \alpha_3 e_3 +$   
 424  $\alpha_4 e_4$ , where  $\alpha_i = 0, 1, i = 1 \dots 4$ .

425 **Property 2** The delineation of a top level 1-cycle that lies  
 426 only on boundaries results in a 1-cycle in the bottom level  
 427 that lies only on boundaries.

428 **Proof:**

429 The process of generator delineation (down-projection)  
 430 presented in [5] requires identifying in the bottom level the  
 431 surviving edges that correspond to the given top level edges  
 432 and where the generator cycles are disconnected, adding  
 433 paths to reconnect.

434 The identified surviving edges are guaranteed to lie on  
 435 boundaries because of their one to one association to their  
 436 corresponding top level edges.

437 As presented in [5], each path added reconnects two con-  
 438 secutive surviving edges, and is a sub-path of the equivalent  
 439 contraction kernel of the common vertex the two surviving  
 440 edges share in the top level. Because

- 441 • for any two vertices in any tree, there is a unique path  
 442 connecting them [21],
- 443 • for any two vertices on the boundary (disconnected end-  
 444 vertices of the two surviving edges) there are two paths  
 445 that connect them and which are made only of boundary  
 446 edges, and
- 447 • boundary edges are never removed [5] (just contracted or  
 448 surviving),

449 we can conclude that the unique path used to reconnect  
 450 the vertices of two consecutive surviving boundary edges is  
 451 made only of boundary edges.  $\square$

## 452 6 Experiments on 2D Images

453 We present and discuss some experiments that have been  
 454 performed on 2D images. We compute homology genera-  
 455 tors, for each region in two different ways: directly on the  
 456 initial image (bottom level), and on the top level of the pyra-  
 457 mid build on this image.

458 One can note that the set of cycles obtained in Fig.5(a)  
 459 and Fig.5(b) do not surround the same (set of) 1D-holes of  
 460 the shape  $S$ . Indeed, these two sets are two different basis of  
 461 the same group  $H_1(S)$ : let  $a, b$  and  $c$  denote the equivalence  
 462 class of cycles that surround respectively the left eye, the  
 463 right eye, and the mouth. The set of generators in Fig.5(a)

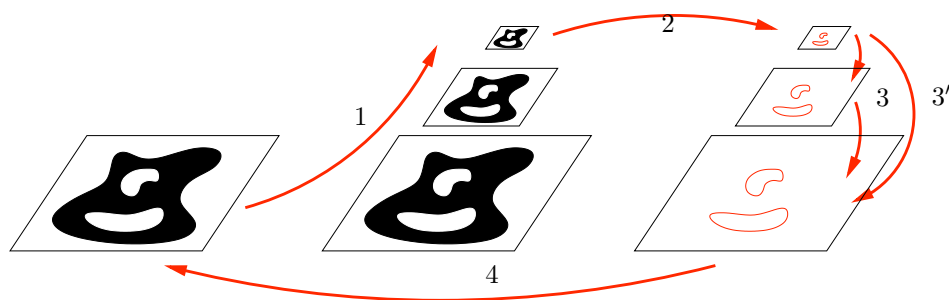


Figure 3: Computing generators of homology groups using an image pyramid.

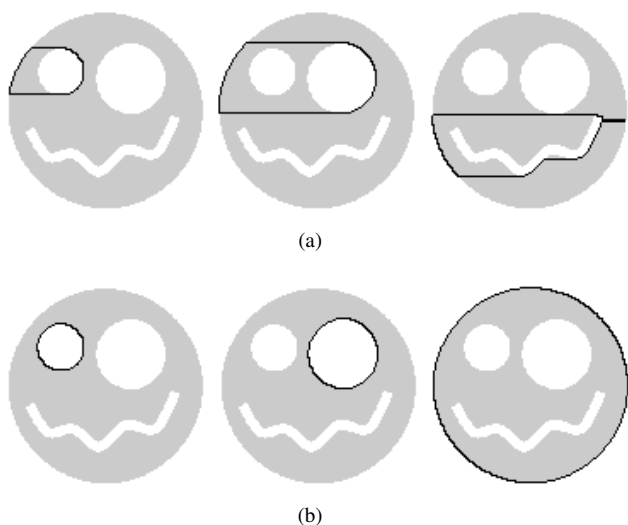


Figure 5: Generators overlaid on the image (a): the homology generators computed on the initial image, (b): GCP generators.

describe  $H_1(S)$  in the basis  $\{a+b, c, a\}$  whereas in Fig.5(b),  $H_1(S)$  is described in the basis  $\{a, a+b+c, b\}$ . Note that in this figure we have put one generators (shown in black) per image.

In Fig.6 and Fig.7 some real world images are shown. We have first segmented the images (e.g. one can choose the minimum spanning tree based pyramid segmentation [7]). In principle one can build generators on these segmented images, but for clarity of this presentation we used binary segmentation (Fig.6(a) and 7(a)). In these binary images white means 1-dimensional hole. Note that for visualization purposes we show with the gray color an island in Fig.6(a) that is not a 1-dimensional hole since it is not enclosed by the black region. The basis in Fig.6(b) and in Fig.6(c) are different but they are basis of the same first homology group. The same holds for images Fig.7(b) and Fig.7(c).

The GCP generators shown in Fig.6(c) and Fig.7(b) are nicely fitted on the boundaries of regions (1D-holes). Note that the generators in Fig.6(b),6(c) and Fig.5(a),5(b) are shown with red and overlaid on the original image.

## 7 Conclusion

The GCP method for computing homology groups and their generators of images, using irregular graph pyramids has the nice property that the build generators always fit on the boundaries of the regions in 2D images. Homology generators are computed efficiently on the top level of the pyramid, since the number of cells is small, and a top down process (down-projection) delineates the homology generators of the initial image. Some results have been shown for 2D binary images.

In future work, we plan to study geometrical properties of homology generators computed with the GCP method for 3D images. In particular, we expect similar properties for homology generators of dimensions 1 and 2 (i.e. tunnels and cavities). We also plan to use these 'geometrically controlled' generators for object matching.

## References

- [1] M. K. Agoston. *Algebraic Topology, a first course*. Pure and applied mathematics. Marcel Dekker Ed., 1976.
- [2] M. Allili, K. Mischaikow, and A. Tannenbaum. Cubical homology and the topological classification of 2d and 3d imagery. In *Proceedings of International Conference Image Processing*, volume 2, pages 173–176, 2001.
- [3] G. Damiand, S. Peltier, and L. Fuchs. Computing homology for surfaces with generalized maps: Application to 3d images. In *Proceedings of 2nd International Symposium on Visual Computing*, volume 4292 of LNCS, pages 1151–1160, Lake Tahoe, Nevada, USA, November 2006. Springer-verlag.
- [4] J.-G. Dumas, F. Heckenbach, B. D. Saunders, and V. Welker. Computing simplicial homology based on efficient smith normal form algorithms. In *Algebra, Geometry, and Software Systems*, pages 177–206, 2003.
- [5] Removed for blind reviewing. Computing homology group generators of images using irregular graph pyramids. Technical report, 2007.
- [6] Damiand G., Peltier P., Fuchs L., and Lienhardt P. Topological map: An efficient tool to compute incrementally topological features on 3d images. In *Proceedings of 11th International Workshop on Combinatorial Image Analysis*, volume 4040, pages 1–15, June 2006.

601 [7] Yil Haxhimusa and Walter G. Kropatsch. Hierarchy  
 602 of partitions with dual graph contraction. In  
 603 B. Milaelis and G. Krell, editors, *Proceedings of German*  
 604 *Pattern Recognition Symposium*, volume 2781 of *Lecture Notes*  
 605 *in Computer Science*, pages 338–345, Germany, 2003.  
 606 Springer.

607 [8] Jean-Michel Jolion and Azriel Rosenfeld. *A Pyramid*  
 608 *Framework for Early Vision*. Kluwer, 1994.

609 [9] T. Kaczynski, K. Mischaikow, and M. Mrozek.  
 610 *Computational Homology*. Springer, 2004.

611 [10] T. Kaczynski, K. Mischaikow, and M. Mrozek.  
 612 *Computational Homology*. Springer, 2004.

613 [11] T. Kaczynski, M. Mrozek, and M. Slusarek.  
 614 Homology computation by reduction of chain  
 615 complexes. *Computers & Math. Appl.*, 34(4):59–70, 1998.

616 [12] R. Kannan and A. Bachem. Polynomial algorithms  
 617 for computing the Smith and Hermite normal forms of  
 618 an integer matrix. *SIAM Journal on Computing*,  
 619 8(4):499–507, November 1979.

620 [13] Vladimir A. Kovalevsky. Finite topology as applied to  
 621 image analysis. *Computer Vision, Graphics, and Image*  
 622 *Processing*, 46:141–161, 1989.

623 [14] Walter G. Kropatsch. Building irregular pyramids by  
 624 dual graph contraction. *IEE-Proc. Vision, Image and Signal*  
 625 *Processing*, 142(6):366–374, December 1995.

626 [15] Peter Meer. Stochastic image pyramids. *Computer*  
 627 *Vision, Graphics, and Image Processing*, 45(3):269–294,  
 628 March 1989. Also as UM CS TR-1871, June, 1987.

629 [16] J. R. Munkres. *Elements of algebraic topology*. Perseus  
 630 Books, 1984.

631 [17] M. Niethammer, A. N. Stein, W. D. Kalies,  
 632 P. Pilarczyk, K. Mischaikow, and A. Tannenbaum.  
 633 Analysis of blood vessels topology by cubical  
 634 homology. In *Proceedings of International Conference Image*  
 635 *Processing*, volume 2, pages 969–972, 2002.

636 [18] S. Peltier, S. Alayrangués, L. Fuchs, and J.-O.  
 637 Lachaud. Computation of homology groups and  
 638 generators. *Computers and graphics*, 30:62–69, february  
 639 2006.

640 [19] Milan Sonka, Václav Hlavac, and Roger Boyle. *Image*  
 641 *Processing, Analysis and Machine Vision*. Brooks/Cole  
 642 Publishing Company, 1999.

643 [20] A. Storjohann. Near optimal algorithms for  
 644 computing smith normal forms of integer matrices. In  
 645 Y. N. Lakshman, editor, *Proceedings of the 1996*  
 646 *International Symposium on Symbolic and Algebraic Computation*,  
 647 pages 267–274. ACM, 1996.

648 [21] K. Thulasiraman and M. N. S. Swamy. *Graphs: Theory*  
 649 *and Algorithms*. Wiley-Interscience, 1992.



(a)



(b)



(c)

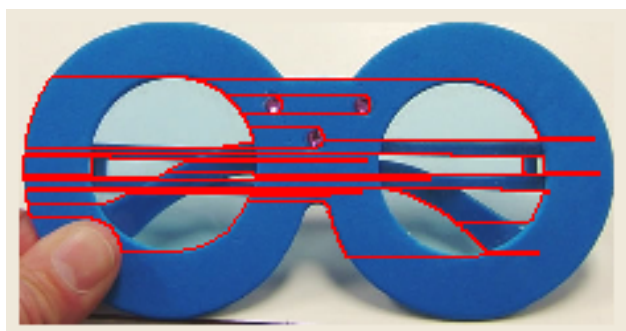
**Figure 6:** (a): segmented image. Generators overlaid on the original image (b): the homology generators computed on the initial image, (c): GCP generators.

721  
722  
723  
724  
725  
726  
727  
728  
729  
730  
731  
732  
733  
734  
735  
736  
737  
738  
739  
740  
741  
742  
743  
744  
745  
746  
747  
748  
749  
750  
751  
752  
753  
754  
755  
756  
757  
758  
759  
760  
761  
762  
763  
764  
765  
766  
767  
768  
769  
770  
771  
772  
773  
774  
775  
776  
777  
778  
779  
780

781  
782  
783  
784  
785  
786  
787  
788  
789  
790  
791  
792  
793  
794  
795  
796  
797  
798  
799  
800  
801  
802  
803  
804  
805  
806  
807  
808  
809  
810  
811  
812  
813  
814  
815  
816  
817  
818  
819  
820  
821  
822  
823  
824  
825  
826  
827  
828  
829  
830  
831  
832  
833  
834  
835  
836  
837  
838  
839  
840



(a)



(b)



(c)

**Figure 7:** (a): segmented image. Generators overlaid on the original image (b): the homology generators computed on the initial image, (c): GCP generators.

841	Document is too long. Maximum of 6 pages is allowed! In	__901
842		__902
843		__903
844		__904
845		__905
846		__906
847		__907
848		__908
849		__909
850		__910
851		__911
852		__912
853		__913
854		__914
855		__915
856		__916
857		__917
858		__918
859		__919
860		__920
861		__921
862		__922
863		__923
864		__924
865		__925
866		__926
867		__927
868		__928
869		__929
870		__930
871		__931
872		__932
873		__933
874		__934
875		__935
876		__936
877		__937
878		__938
879		__939
880		__940
881		__941
882		__942
883		__943
884		__944
885		__945
886		__946
887		__947
888		__948
889		__949
890		__950
891		__951
892		__952
893		__953
894		__954
895		__955
896		__956
897		__957
898		__958
899		__959
900		__960

961__	Document is too long. Maximum of 6 pages is allowed! In	_1021
962__		_1022
963__		_1023
964__		_1024
965__		_1025
966__		_1026
967__		_1027
968__		_1028
969__		_1029
970__		_1030
971__		_1031
972__		_1032
973__		_1033
974__		_1034
975__		_1035
976__		_1036
977__		_1037
978__		_1038
979__		_1039
980__		_1040
981__		_1041
982__		_1042
983__		_1043
984__		_1044
985__		_1045
986__		_1046
987__		_1047
988__		_1048
989__		_1049
990__		_1050
991__		_1051
992__		_1052
993__		_1053
994__		_1054
995__		_1055
996__		_1056
997__		_1057
998__		_1058
999__		_1059
1000__		_1060
1001__		_1061
1002__		_1062
1003__		_1063
1004__		_1064
1005__		_1065
1006__		_1066
1007__		_1067
1008__		_1068
1009__		_1069
1010__		_1070
1011__		_1071
1012__		_1072
1013__		_1073
1014__		_1074
1015__		_1075
1016__		_1076
1017__		_1077
1018__		_1078
1019__		_1079
1020__		_1080